Evaluation of the Performance and Economic Viability of a Novel Low Temperature Carbon Capture Process

Paul Willson[a], George Lychnos[a], Alastair Clements[b], Stavros Michailos[b], Carolina Font-Palma[c*], Maria Elena Diego[b], Mohamed Pourkashanian[b], Joe Howe[c]

[a]*PMW Technology Limited, Thornton Science Park, Ince, Chester, CH2 4NU*
[b]*Energy 2050, Faculty of Engineering, University of Sheffield, S10 2TN, UK*
[c]*Department of Chemical Engineering, Thornton Science Park, University of Chester, Chester, CH2 4NU, UK*

Abstract

A novel Advanced Cryogenic Carbon Capture (A3C) process is being developed using low cost but high intensity heat transfer to achieve high CO_2 capture efficiencies with a much reduced energy consumption and process equipment size. These characteristics, along with the purity of CO_2 product and absence of process chemicals, offer the potential for application across a range of sectors. This work presents a techno-economic evaluation for applications ranging from 3% to 35%vol. CO_2 content. The A3C process is evaluated against an amine-based CO_2 capture process for three applications; an oil-fired boiler, a combined cycle gas turbine (CCGT) and a biogas upgrading plant. The A3C process has shown a modest life cost advantage over the mature MEA technology for the larger selected applications, and substantially lower costs in the smaller biogas application. Enhanced energy recovery and optimization offer significant opportunities for further reductions in cost.

Keywords: low temperature; carbon capture; anti-sublimation; desublimation; cryogenic separation

1. Introduction

Current advances in existing and emerging CO_2 capture and storage (CCS) technologies are mostly driven by the need for reductions in the energy penalty and costs of CCS to make it more attractive for commercial deployment. Amongst these technologies, low temperature CO_2 separation has been considered as an option for capturing CO_2 from process gas streams. This process relies on phase change, thus separating the CO_2 from the gas in the form of liquid or solid (Berstad et al., 2013). Unlike amine-based processes, these low temperature systems avoid the use of chemical absorbents and deliver a high-purity dry CO_2 stream as product. Despite these advantages, low temperature CO_2 separation is often considered to be a highly-energy consuming alternative, mainly due to the cooling duty required (Berstad et al., 2013; Tuinier et al., 2011a). Desublimation processes separate CO_2 as a solid frost at conditions below the sublimation temperature (195 K at 1 bara). The CO_2 frost is then warmed to sublimation conditions to release a pure CO_2 stream for reuse or storage. Unlike cryogenic processes that separate CO_2 in the form of a liquid, desublimation systems avoid energy-intensive raw gas compression stages by operating at close to atmospheric pressure. Moreover, desublimation processes can achieve CO_2 capture ratios of virtually 100% and remove both water and CO_2, thus avoiding the need for product drying stages (Berstad et al., 2013; Clodic and Younes, 2002; Tuinier et al., 2010). Effective integration with a refrigeration system or low-cost cold source to meet the need for cooling is essential for the competitiveness of these processes (Tuinier et al., 2011a).

Research groups from the Ecole de Mines de Paris (Clodic et al., 2005a; Clodic and Younes, 2002; Clodic et al., 2005b; Clodic et al., 2011), Eindhoven University of Technology (Tuinier et al., 2011a; Tuinier et al., 2010; Tuinier et al., 2011b), Brigham Young University (Burt et al., 2009) and Tianjin University (Song et al., 2017) have investigated the concept of desublimation for CO_2 separation and proposed novel configurations. Clodic et al. proposed a cryogenic system that uses a refrigeration

* Corresponding author. Tel.: +44(0) 1244 512377; fax: +44(0) 1244 511300.
E-mail address: c.fontpalma@chester.ac.uk

cascade for CO_2 separation. This process requires water removal prior to the CO_2 capture stage to avoid issues related to ice formation. Then the CO_2 is deposited as a frost layer on the surface of a low temperature frosting evaporator (Clodic et al., 2005a; Clodic and Younes, 2002). However, this hinders heat transfer as the CO_2 layer is deposited, thus reducing process efficiency (Tuinier et al., 2010). Advanced configurations using packed beds have been developed to overcome this issue (Tuinier et al., 2011a; Tuinier et al., 2010; Tuinier et al., 2011b). These systems can separate both water and CO_2 on the packing surface, without the need for additional drying stages. They are based on a cycle of bed cooling, CO_2 capture and sublimation processes. The flue gas is fed to a chilled bed, where the water contained in the flue gas condenses, the flue gas cools down further and the CO_2 desublimation process begins (Tuinier et al., 2011a). Once the CO_2 desublimation front reaches the last part of the bed, the cycle steps to sublimation by feeding a warm CO_2 stream through the bed. Finally, the bed is cooled down with a low temperature gas prior to a new cycle of desublimation. Both the freezing evaporator and packed bed systems require periodic switching between CO_2 capture, sublimation and bed cooling conditions. The use of multiple parallel beds permits such processes to operate continuously (Tuinier et al., 2011a; Tuinier et al., 2010). However, the energy consumption of these processes is high, necessitating the availability of a low cost cold source, such as the evaporation of liquefied natural gas (Tuinier et al., 2011a). Indeed Tuinier et al. (2011a) concluded that the use of external refrigeration for such a process for carbon capture on a power plant would consume its entire power output. Song et al. (2012), proposed the use of Stirling coolers to provide the cooling requirement for condensing moisture, desublimation of CO_2 and maintaining storage conditions of the dry ice (Song et al., 2017).

In applications where biogas is purified and converted to bio-LNG at low temperatures, low-temperature distillation and desublimation processes can be applied (Pellegrini et al., 2018). The separation of CO_2 is necessary prior to liquefaction of methane, with the separation and liquefaction processes being closely integrated in the cases considered by Pellegrini et al. (2018). The additional carbon dioxide removal processes identified are based on low temperature distillation at elevated pressures.

This paper presents a novel cryogenic process aimed at reducing the energy consumption and costs of CO_2 separation. The A3C process described in this paper is subject to a recent UK patent application (Willson, 2016). The process overcomes some limitations of previous cryogenic systems by using a moving bed of metallic beads as a heat transfer medium and frost capture surface. This achieves intensive heat transfer while avoiding the adverse effects of heavy frost deposition. The process eliminates the need for multiple beds and associated switching losses to offer a much reduced energy consumption and process equipment size. This work details the process concept and evaluates its performance and life cost for a range of process gases containing from 3% to 35%vol. CO_2.

2. The A3C Separation Process

The A3C separation process has two stages, each with a circulating packed bed of 1-5 mm diameter metallic beads. These are a cooling-drying step, and a CO_2 separation step, as shown in figure 1. The quenched raw gases are cooled conventionally to 274K to condense most of the water vapour. The residual water content is removed as frost in the cold end of the first circulating packed bed, where the water ice deposition is typically 0.1% of the bed mass flow rate. By cooling to 174 K, the water content of the gas is reduced to below 50 ppb. The frost bearing bed is carried out of the raw gas stream, warmed slightly to melt the ice and transferred to a section where it moves in counterflow to the lean gas leaving the desublimation step in the core process. The warm moist bed is dried and cooled by the cold dry lean gas stream. Supplementary refrigeration compensates for the removal of the carbon dioxide from the lean gas. The cold bed is returned at a low temperature to the raw gas section.

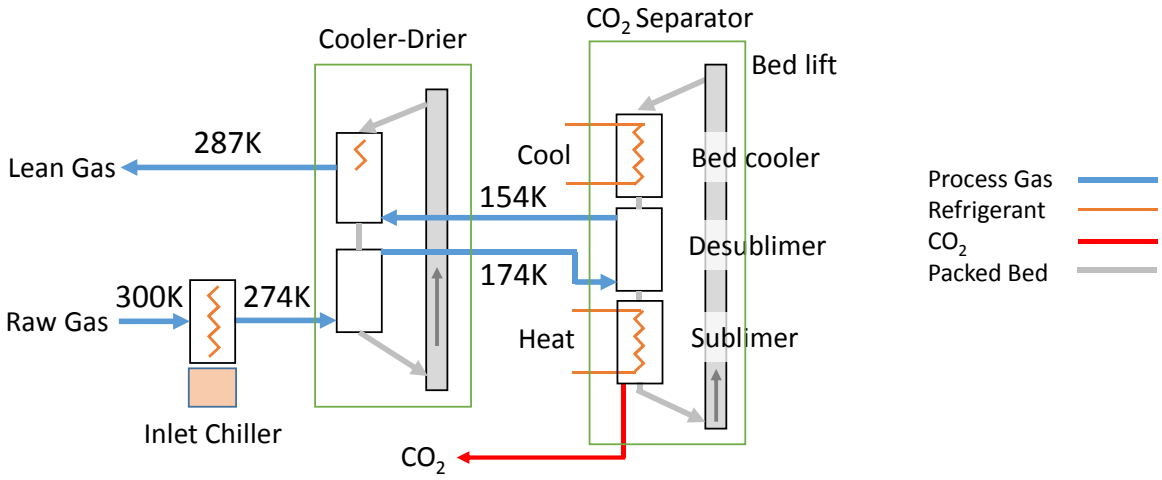

Fig. 1. Outline of the two stages of the A3C CO_2 separation process. Temperatures refer to the oil-fired boiler application.

The cold dry gas is passed into a second circulating packed bed cascade of similar design to the cooler-drier. In the desublimer, it flows counter to a colder bed, so that the CO_2 in the gas stream deposits as a frost on the bed material. The lowest gas temperature, around 150K, is chosen to correspond to the CO_2 saturation temperature at the desired residual content. The bed carries the CO_2 frost to the gas inlet end of the bed and through a gas lock into the sublimer heat exchanger where it is warmed to about 200K to recover the CO_2 by sublimation. The mass flow of CO_2 frost is typically around 1% of the bed mass flow rate. The frost-bed is then cooled in the refrigerated bed cooler to the desired inlet temperature.

The A3C CO_2 separation process has many analogous features to distillation. The desublimation stage has a temperature gradient from lower at the top to higher at the bottom with conditions selected so that the vapour pressure of the desubliming bottom product is in equilibrium with its partial pressure in the gas phase. The gases flow upwards in intimate contact with a falling stream of colder solid phase, carried on a reflux of cold inert bed material. The reflux of bed material is cooled, as in an overhead condenser and the bottom product is recovered by sublimation with heating. These analogies are reflected in identical heat, mass and continuity equations to those for a conventional distillation column replacing enthalpies of vapourisation with enthalpies of sublimation.

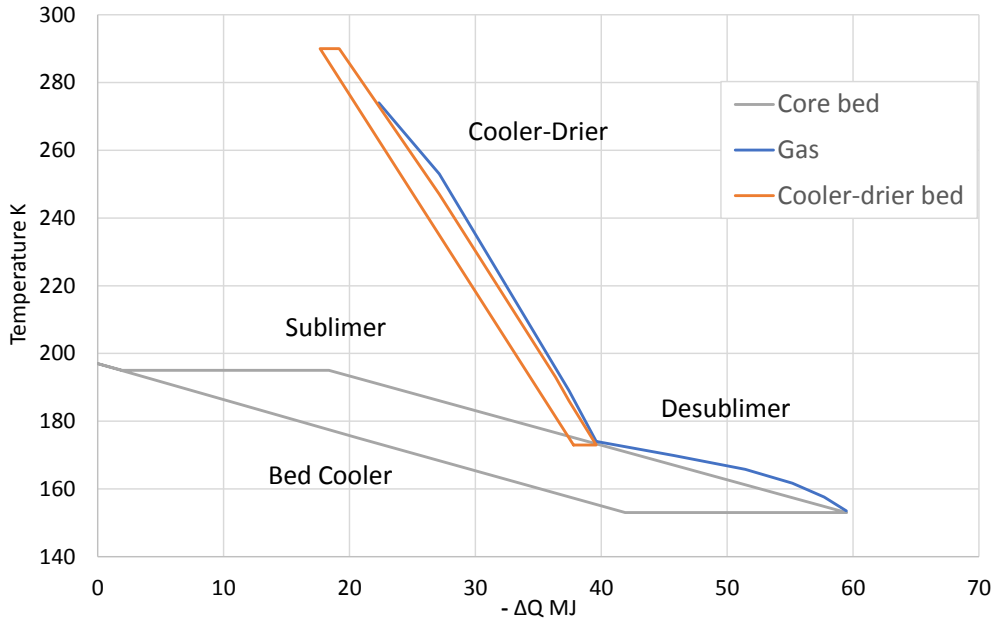

Fig. 2 Q-T Diagram for the A3C separation process for an oil-fired boiler application.

Figure 2 illustrates the Q-T diagram of the A3C separation process for an oil-fired boiler application (12.18%vol CO_2 in the flue gas). It shows the variation of temperature and energy of the inlet gas and the circulating beds, as they are cyclically heated and cooled. The raw gas (blue line) is first cooled and ice is captured as frost on the cooler-drier bed (orange line). The dry raw gas is further cooled by the core bed (grey line) to the point where 90% of the CO_2 is desublimed. As it flows beyond the gas inlet the circulating bed of the cooler-drier is heated further to evaporate the condensed water. From its lowest temperature the core bed is first warmed by the desublimation of the incoming CO_2. Separated from the inlet gases, the bed is then warmed further with heat rejected by the refrigeration system. When its temperature reaches 195K the CO_2 is sublimed off the bed, with a small overshoot in temperature to ensure complete sublimation. The bed is then cooled by refrigeration for return to the desublimer.

The A3C refrigeration system uses conventional refrigeration components but it is unusual in that it provides cooling to a low temperature (around 150 K for the oil-fired boiler case) and rejects heat at two higher temperatures, to the sublimer at 180-205 K and to ambient conditions at 290-320 K. Aspen modelling confirms that this refrigeration configuration achieves a coefficient of performance (COP) of significantly over unity compared with a conventional cascade refrigeration system which would achieve a COP of around 0.4 for cooling to the same lower temperature (Berstad et al., 2013; Davidson, 2007; Podtcherniaev et al., 2002). This refrigeration system contributes strongly to the energy efficiency of the A3C process.

2.1. A3C Modelling and analysis

Deriving data for benchmarking the A3C process against an absorption-based carbon capture process required the modelling of the process behaviour and energy performance, preliminary engineering of the process equipment and the costing of the equipment. Each of these steps was repeated for the selected applications; an oil-fired boiler, a combined cycle gas turbine (CCGT) and a biogas upgrading plant.

Modelling the thermodynamic behavior of the A3C process in Aspen Plus® presented several challenges. The capture of CO_2 at atmospheric pressure and low temperatures necessitates the process gas to be cooled down to the sublimation temperature, which is set by the partial pressure of the CO_2 (Clodic et al., 2005a). Hence one of the challenges was to find a way to represent the phase equilibria behaviour. In the A3C process, there is a phase change between gaseous CO_2 and solid CO_2 and vice versa. The function library of Aspen Plus® only includes the RGibbs block to handle vapour-solid equilibria calculations, while differentiating between solid and gaseous CO_2. Heat and mass transfer effects are not evaluated in this block, as it only simulates the phase equilibria and calculates the energy change taking place in the process gas stream for a defined temperature change. The progressive CO_2 desublimation in the moving bed was therefore represented by small steps, each frosting over a small temperature range (an average of typically 4 K), similar to the approach of Schach et al. (2011). The number of steps affects the accuracy of representation of the energy consumption of the progressive process. Ten equal temperature steps were found to be adequate by Schach et al. (2011), but in this study five steps were found to achieve adequate accuracy. Aspen Plus® provides no blocks for modelling heat and mass transfer between a moving solid bed and gases so an analogous representation had to be developed. In this work, the solid bed was represented by a liquid, with the direct contact heat exchange in the bed represented by indirect heat exchange. The carbon dioxide or water deposition on the bed was then represented by mixing the respective solid with the counter-flow of liquid after each stage of frosting, and sublimation or melting was represented by separation of the gaseous or immiscible water phase from the liquid representing the bed. The liquid for each stage was selected to be non-reactive with water or carbon dioxide respectively and to remain liquid across the temperature range of the stage. Heptene was selected for the first stage and dimethyl ether for the second. The flow rates of the liquid analogues were scaled from the ratio of specific heats with the stainless steel bed material considered here. The validity of these representations was checked separately by a spreadsheet model of the core process using a solid

moving bed. This model used a finite temperature step representation of 1K, applying conservation of energy and mass for each step through the heat and/or mass exchange processes. Accurate low temperature gas properties were used from (Jäger and Span, 2012; Lemmon et al., 2018). This check demonstrated alignment of the alternative representations within the uncertainty of convergence of the models.

The Aspen Plus® model consists of two sub-models, the cooler-drier and the core-fridge, that are combined and interact through a Microsoft® Excel file using the Aspen Simulation Workbook. Through an iterative sequential procedure, starting from the core/fridge model balanced using the sensitivity analysis tool and then followed by the cooler-drier, the solution is achieved when the variables (mass flow and temperature) converge to the target values with less than 1% absolute temperature error. Each model has two basic distinct stream flows i.e. the process gas stream and the bed stream that interact with each other via Heat Exchanger blocks (HeatX or MHeatX). The core/fridge sub-model has an extra stream representing the refrigerant flow coming from the refrigeration system which incorporates a multi-stage compressor and several heat exchangers.

Preliminary engineering of the process exploited the capability of the Aspen Plus® Process Economic Analyser (APEA) to size and cost the conventional heat exchangers and components such as the CO_2 compressor. The APEA estimates the cost of the process equipment by correlating modelled results and parameters with data from vendors, and is often used for preliminary costing analysis (Husebye et al., 2012; Jung et al., 2013; Roussanaly et al., 2017). However, this approach was limited by the representation of the bed as a liquid and by the vapour-solid phase changes in the desublimer, sublimer and cooler-drier heat exchangers being represented by cascades of RGibbs blocks in the model. Since neither the heat exchangers to the moving packed bed nor the heat and mass transfers within the beds can be considered to be conventional heat exchangers, an alternative approach to the heat exchanger design and costing was necessary. The heat transfer areas were calculated manually based on the duties and approach temperatures given by the Aspen model for these exchangers, with appropriate heat transfer coefficients derived from other sources (Achenbach, 1995; Colakyan, 1985). The direct contact bed heat exchangers were sized to limit gas velocities to below 70% of that necessary for fluidization and costed by analogy with fixed packed bed vessels of similar dimensions, based on data from Aspen Plus®. Some of the bed heat exchangers, such as for bed cooling prior to the desublimation step, need to use unconventional exchangers using tubes submerged within the moving bed. The application of such exchangers for coarse bed material is not well described in literature and tube sizing and arrangements similar to those for shell and tube exchangers with a single pass on the shell side and multiple passes on the evaporation side were assumed to be a reasonable approximation. The costs of comparable heat exchangers from Aspen Plus® were used as the basis for cost estimates for these exchangers.

It is worth noting that for the Biogas Upgrading case reduced multipliers were used for construction expenses due to factory and skid assembly for the A3C unit which has a footprint of approximately 2m x 3m.

Establishing a cost estimate for a novel technology using established process equipment types is challenging, being sensitive to a range of technical and commercial factors that limit the confidence in the result of any estimation methodology. For some high cost elements which use established technology, costs can be better estimated, but for new equipment types of the A3C process there is larger technical and cost uncertainty. Based on the cost estimate classification system by the Association for the Advancement of Cost Engineering (AACE), the costs presented here regarding the A3C process are no better than class 5 (concept screening) with an expected accuracy range of no less than +50%/-30%.

2.2. Applications evaluated

The A3C process was compared with a reference amine case for three applications, namely oil-fired boiler, a combined cycle gas turbine (CCGT) and a biogas upgrading plant, which offered a

range of scale and CO_2 content of the process gases. To achieve the conventional 90% capture rate for the fired boiler and CCGT, the flue gas was cooled down to 154 K and 144 K, respectively, for the A3C process. For unrestricted injection of biogas into the UK gas grid a 3%vol. maximum CO_2 content is necessary. For this application the biogas was cooled to 159 K to deliver the 94% capture rate needed, since the raw biogas CO_2 concentration is 35 %vol.

A common basis of inlet conditions for process gases was applied for the comparison, as detailed in Table 1, with CO_2 delivery at 110 bar supercritical and dry to better than 1 ppm to meet conventional transport and storage requirements (Vattenfall, 2008); (IEAGHG, 2011).

Table 1: Key process gas inlet conditions for the three application cases.

	Oil Fired Boiler	CCGT	Biogas upgrading
Power generation (MW)	125	60	-
Gas flow rate (t/h)/(kNm^3/h)	612 / 472	493 / 388	0.83 / 0.77
CO_2 content (vol. %)	12.18	3.23	35
N_2 (vol. %)	76.16	75.87	-
O_2 (vol. %)	-	13.84	-
H_2O (vol. %)	11.66	7.06	-
CH_4 (vol. %)	-	-	65
Capture rate (%)	90	90	94
CO_2 capture rate (t/h)	103.7	20.7	0.45

2.3. Reference case

The use of amine-based CO_2 capture systems is widely seen as the most market ready CCS technology, due to the application at commercial scale (Stéphenne, 2014) and pilot/demonstration scale plants (Akram et al., 2016; Knudsen et al., 2009; Seibert et al., 2011; Strazisar et al., 2003) in operation, and due to the technology's long standing in other chemical processes to strip CO_2 (Rabensteiner et al., 2014), which makes it a suitable technology for the reference case. In this study the process layout presented by Metz et al. (2005) was adopted, using a conventional 30 wt.% MEA solvent as a benchmark. The amine plant was modelled in Aspen Plus® in order to determine the necessary thermal and electrical duties of the plant, as well as estimate the required sizes of the unit components, which are necessary for the costing analysis.

The lean and rich pumps, which are responsible for the electrical power requirement of the amine plant, were modelled with an efficiency of 80%, and were configured to provide an outlet pressure to provide a desired pressure within the absorber and stripper columns, taking into account the hydrostatic pressure drop incurred to pump the solvent to the top of the columns. The absorber column was expected to be at atmospheric pressure at the top of the column, while the pressure at the bottom of the stripper column was maintained at a level to provide an optimal lean loading, while the reboiler temperature was fixed at 393 K, which has been recommended to reduce solvent degradation (Gouedard et al., 2012). The column diameters were calculated to provide a gas velocity that was 80% of the flooding velocity; with the flooding velocity, as well as mass transfer and pressure drop, calculated using the correlations by Billet and Schultes (1993). The absorber and stripper column heights were sized to achieve the desired CO_2 capture rate for each case and to minimise the specific reboiler duty, respectively. The solvent cross heat exchanger was sized to raise the temperature of the rich solvent to 363 K, assuming a constant heat transfer coefficient of 600 W/m^{2}K. A reclaimer system is required to prevent the accumulation of degraded amine waste in the circulating solvent. The adopted design in this study assumes that the reclaimer slipstream is purged on the discharge section of the lean solvent pump and the reclaimed amine returns on the suction section of the lean solvent pump. The mass balance considers a slipstream of 0.1 wt.% of the total circulation rate (Sexton et al., 2014).

The compression section was modelled as three compressors with intermediate cooling, followed by a pump and a final cooling stage. As low moisture content is critical in prevention or minimization

of both corrosion and solid hydrates formation, a typical molecular sieve configuration was considered here with the aim of reducing water concentration to below 1 ppm in the dried gas.

Aspen APEA has been utilised to estimate the direct equipment costs (DEC) based on equipment sizing derived from the simulations of the MEA reference case. Evaluation of the total capital requirement followed the common costing methodology detailed in Table 2.

2.4. Levelised cost of carbon capture (LCCC)

A cost model based on conventional methods was used to produce a levelised cost of carbon capture (LCCC) for the reference and A3C cases for the three applications. The LCCC excluded the costs of transport and storage or for carbon emission credits. The model used consumptions of heat, power and MEA make-up derived from the respective process models. Common unit costs of heat, power and MEA were applied to derive A3C and reference case operating costs while fixed costs were estimated from capital costs, as indicated in Table 3. LCCC is reported in constant monetary values meaning that inflation effects are excluded. This approach is suitable for preliminary design studies and technology comparisons since it encapsulates existing market conditions and offers a more legitimate picture of actual cost trends without the probable distortions caused by inflation effects over many years (Rubin et al., 2013). The LCCC is given as

$$LCCC = \frac{TCR \times FCF + FOM}{CF \times \dot{m}_{CO2}^{cap}} + VC \quad (1)$$

where TCR is the total capital requirement, FCF is the fixed charge factor, FOM fixed operating & maintenance costs, CF is the capacity factor, $\dot{m}_{CO2}^{cap}$ is the annual CO_2 capture rate and VC stands for variable costs. As denoted in Eq.(1) the FCF is actually the levelisation factor for the TCR. It is used to convert the TCR into a uniform annual amount and it is calculated as a function of the discount rate, r, and the lifetime of the project, n years

$$FCF = \frac{r \times (1+r)^{\mathrm{n}}}{-1+(1+r)^{\mathrm{n}}}$$

A discount rate of 10% was used as it constitutes a conventional and legitimate market assumption while the project lifetime was assumed to be 15 years, as the current cases are considered as retrofit applications, and the capacity factor was assumed to be 85%.

Early stage CAPEX estimates are commonly based on the DEC, with all additional cost elements being appraised by means of explicit default factors, i.e. specific percentages of the DEC (comprises purchased equipment cost along with installation costs). The full methodology applied to both the A3C and MEA reference cases is tabulated in Table 2.

Table 2. CAPEX estimation methodology

	Item	Method	References
A	Equipment Cost	Aspen Cost Estimator	-
B	Installation Factor	Aspen Cost Estimator	-
C	**Direct Equipment cost (DEC)**	**∑Ai×Bi i=1, n**	-
D	Construction Expenses	0.34×DEC	(Peters and Timmerhaus, 1991)
E	Legal Expenses	0.04×DEC	(Peters and Timmerhaus, 1991)
F	Contractor's Fee	0.19×DEC	(Peters and Timmerhaus, 1991)
G	Indirect Equipment Cost	D+E+F	-
H	**Inside Battery Limit Investment (ISBL)**	**C+G**	-
I	Off sites (OS)	0.15×ISBL	(Towler and Sinnott, 2013a)
J	Process unit investment (PUI)	ISBL + OS	-
K	Engineering	0.12×PUI	(Alhajaj et al., 2016; Chauvel Alain, 1976)

L	Paid up royalties	0.07×ISBL	(Chauvel Alain, 1976)
M	Project Contingency	0.15× (ISBL+OS)	(Couper, 2003)
N	Process Contingency	0.05× (ISBL+OS)	(Couper, 2003)
O	**Fixed Capital Investment (FCI)**	**PUI+K+L+M+N**	-
P	Start up + MEA costs	0.1×FCI	(Peeters et al., 2007)
Q	Interest during construction	Computed	
R	**Total Capital Requirement (TCR)**	**O+P+Q**	-
S	Working Capital	0.05×FCI	(Towler and Sinnott, 2013a)

The fixed capital investment was assumed to be spent over a 3-year construction period, with 10% in the first year, followed by 60% and 30% for the second and third years respectively. Working capital was applied in the year before operation and recovered at the end of the plant life (therefore, it was not depreciated).

Table 3 lists the chief components of the OPEX applied to both the A3C and reference cases. These comprise variable and fixed costs. The former expenditures refer to utilities and MEA costs while the latter consist of labour, supervision, direct salary overhead, maintenance, insurance and general plant overhead.

Table 3. Elements to estimate FOM and VC

	Basis	Value/Multiplier	References
Fixed operating & maintenance (FOM)			
Operating labour (OL)	£/y	53,700	(BEIS, 2018)
Operating supervision	OL	0.15	(Albrecht et al., 2017; Peters and Timmerhaus, 1991)
Maintenance labor (ML)	TLC FCI	0.015	(Albrecht et al., 2017; Peters and Timmerhaus, 1991)
Maintenance material (MM)	FCI	0.015	(Albrecht et al., 2017; Peters and Timmerhaus, 1991)
Operating supplies	ML+MM	0.15	(Albrecht et al., 2017; Peters and Timmerhaus, 1991)
Insurance and taxes	FCI	0.02	(Albrecht et al., 2017; Peters and Timmerhaus, 1991)
Plant overhead costs [PO]	TLC	0.6	(Albrecht et al., 2017; Peters and Timmerhaus, 1991)
Administrative costs	PO	0.25	(Albrecht et al., 2017; Peters and Timmerhaus, 1991)
Financing working capital	WC	0.1×WC	(Towler and Sinnott, 2013b)
Variable Costs			
Electricity	£ MWh^{-1}	42.06*	
Cooling water	£ kg^{-1}	2.51E-05	(Towler and Sinnott, 2013b)
MEA make up	£ kg^{-1}	1.03	(Alhajaj et al., 2016)

*average wholesale electricity price over the last 3 years

For the reference case the operators' labour requirement was calculated by employing the following correlation (Turton, 2009):

$$N_{OL} = (6.29 + 31.7P^2 + 0.23N)^{0.5} \quad (3)$$

where P is the number of solids handling steps and N is the number of non-particulate processing steps. A process step is defined as any unit operation or unit process or even combination that takes place in one or more units changing the chemical composition or thermodynamic state of the participating process streams significantly. For each of the N_{OL} (3 in total) operators per 8-hour shift, approximately four operators must be hired for a plant that runs 24 hours per day, to account for three shifts per day as well as regular and sick annual leaves (Iijima, 1998).

For the A3C case, it was assumed that as the process was mechanical and thermal in nature and was an addition to an existing process plant, it would require limited additional attention and supervision. It was assumed that a single operator per shift would be required for the larger oil-fired boiler and gas turbine cases and a part-time operator per shift for the biogas case would be needed. For both A3C and reference cases an average annual salary cost of £53,700 was used (BEIS, 2018).

In this work the cost of supplying heat to the system was appraised as an opportunity cost due to the lost electricity generation (and subsequently revenues) from steam bleed to reboiler. In order to convert thermal to electrical energy, a factor that lies in the range of 20% and 25% is suggested for retrofit designs (Rao et al., 2004); a value of 24% is adopted in the present study for the heat-to-electricity equivalence factor, which relates to the thermal duty being extracted from the low pressure steam section. Alternative costs of heat can be justified for different situations, for example where surplus low temperature steam is available, but these have not been analysed here.

3. Results and Discussion

3.1. Comparison of the processes

The results of modelling the A3C and reference cases include estimates of flows, heat exchange duties and the power consumption of fans, pumps, compressors and ancillary items for the respective processes. Only a limited breakdown will be given for the MEA cases while more comprehensive data will be presented for the A3C cases.

3.2. Outline of MEA cases

The heat and power consumption of the reference MEA implementations for the three applications are detailed in Table 4 together with the lost opportunity equivalent power consumption of the LP steam supplied to the process.

Table 4: The reference MEA energy consumption breakdown for the three applications

Energy consumer	**Units**	**Oil-fired Boiler**	**CCGT**	**Biogas Upgrading**
LP steam for stripper	MWth	114.0	28.6	0.49
Lost opportunity equivalent electricity	MWe	27.4	6.9	0.12
Process pumps	MWe	1.23	0.63	0.0015
Reclaimer and PSA	MWe	0.77	0.29	0.0035
CO_2 delivery compressor	MWe	10.19	2.03	0.059
Total Equivalent consumption	MWe	39.59	9.85	0.184
Total specific energy of CO_2 capture	kWh/tonne	382	476	397
Specific energy of CO_2 separation	kWh/tonne	284	378	269
Cooling water utility requirement	MWth	154	39	0.67

The physical sizing and rating data for the various plant elements in the reference MEA cases derived from the analysis and modelling are detailed in Table 5. The largest column size is required for the absorber of the oil-fired boiler case, as this case deals with the largest volume of flue gas, with the absorber diameter being 9.9 m, which is comparable to results from similar studies (Nwaoha et al.,

2018). At large scales, amine capture plants will be designed with two columns to avoid oversized units and provide operating flexibility, however the columns for these cases are smaller than units typically designed for two-absorber column capture plants on industrial scale plants (Agbonghae et al., 2014; Diego et al., 2018), so a one-absorber design was maintained for consistency throughout the cases.

Table 5: Summary of the reference case designs

	Units	Oil-fired Boiler	CCGT	Biogas Upgrading
Absorber column height	m	17.9	11.18	11.5
Absorber column diameter	m	9.9	6.9	0.7
Stripper column height	m	18.5	13.86	9.5
Stripper column diameter	m	6.2	2.68	0.45
MEA solvent flow rate	kg/s	521	133	2.55
Rich pump outlet pressure	kPa	423	380	420
Lean pump outlet pressure	kPa	349	290	320
Cross heat exchanger area	m^2	4575	1185	14

Costs of the MEA reference cases are detailed in Table 6. These have been derived from the Aspen cost analysis and the use of the CAPEX methodology detailed in Table 2.

Table 6: The cost breakdown for the MEA cases for the three applications

Cost Element £k	Oil-fired boiler	CCGT	Biogas upgrading
Direct equipment cost process	19,960	9,065	877.6
Direct equipment cost CO_2 compression	7,457	3,577	606.5
Total DEC	27,417	12,642	1,484.1
Total fixed capital investment	68,355	31,520	3,700.2
Start-up and MEA	6,835	3,152	370.0
Interest during construction	6.090	2,808	329.7
Total Capital Requirement	81,280	37,480	4,899.9

3.3. A3C analysis results

The breakdown of key features of the A3C cases is given in Table 7 which lists the duties and required heat exchange areas by type for the core-fridge and cooler-drier elements. A significant number of individual exchangers make up the total in the fluid to bed category with none of these being of exceptional duty or area. The conventional exchangers are dominated by the duty and area required for the recuperative heat exchanger in the refrigeration system. Since this is likely to be a brazed plate exchanger or similar compact unit, the large areas required are feasible at reasonable cost. The direct bed heat exchangers in the cooler-drier and desublimer have large areas but with a typical bed material of 1.5 mm diameter beads offering a surface area of 2400 m^2/m^3, these are compact and economical.

Table 7: Core-Fridge, Cooler-Drier heat exchange duties and areas for A3C in the three selected applications

	Oil-fired Boiler		CCGT		Biogas upgrading	
Core-Fridge	**Duty MW**	**Area m^2**	**Duty MW**	**Area m^2**	**Duty kW**	**Area m^2**
Conventional HX	24.9	13,400	13.0	21,400	68.2	34.7
Fluid to bed HX	81.5	33,900	36.5	11,400	234.6	110.4
Direct bed to gas HX	19.9	24,800	5.3	6,700	81.2	101.5
Refrigeration cooling	44.1		21.1		114.5	
Cooler-Drier						

Fluid to bed HX	5.32	1,100	2.62	684.5	13.1	3.27
Direct bed to gas HX	31.3	28,400	24.3	27,000	51.4	83.5

Preliminary engineering of the A3C process for each of the applications derived bed material flow rates and physical size estimates for the equipment. The bed material flow rates for the core process for the respective applications were 0.55 m^3/s, 0.19 m^3/s and 0.002 m^3/s. A significant finding was that the direct contact heat and mass transfer in the moving packed beds was intense while the superficial gas flow rates through the beds were limited to typically around 1m/s. The consequence of this finding is that the depth to diameter ratio of the beds is typically very low, with bed depths of 80-160 mm while bed diameters of up to 10 m are necessary for the larger applications. Two issues arise from this; maintaining a consistent bed depth across wide shallow beds will require special bed distribution arrangements, while ensuring mass flow of material vertically though the beds will necessitate multiple outlets so that the height of material over each outlet does not exceed its diameter, to satisfy the criterion for mass flow. The distribution of material across large diameter moving packed beds has been addressed successfully in the malting industry, where malt kilns of up to 20 m in diameter are widely used, albeit with greater bed depths (Don Valley Engineering, 2018). The need for multiple bed outlets increases the complexity of construction but has the benefit of minimising the quantity of 'idle' bed material in the deep vessel outlet hoppers that would otherwise be necessary.

The physical arrangement of wide but shallow beds and bed heat exchangers in the cooler-drier and core processes lends itself to stacking of the components with the bed material flowing by gravity through the successive sections, with the circulation of the bed material being achieved by bed lifts, potentially bucket elevators, located around the periphery of the vessels. Such an arrangement is illustrated in Figure 3, showing the relatively compact layout. The core process vessel is about 7m high with the bed lifts being about 12m high to allow for gravity bed flow above and below the vessel.

Another challenge discovered during the preliminary engineering phase was the arrangement of the cooler-drier bed to ensure that the moisture captured on the bed was evaporated and carried out by the lean gases. The analysis of the Q-T chart for the process showed that preheating the moist bed using low grade waste heat at less than 300 K, from another section of the process, assured proper bed dry-out before it was returned to be cooled.

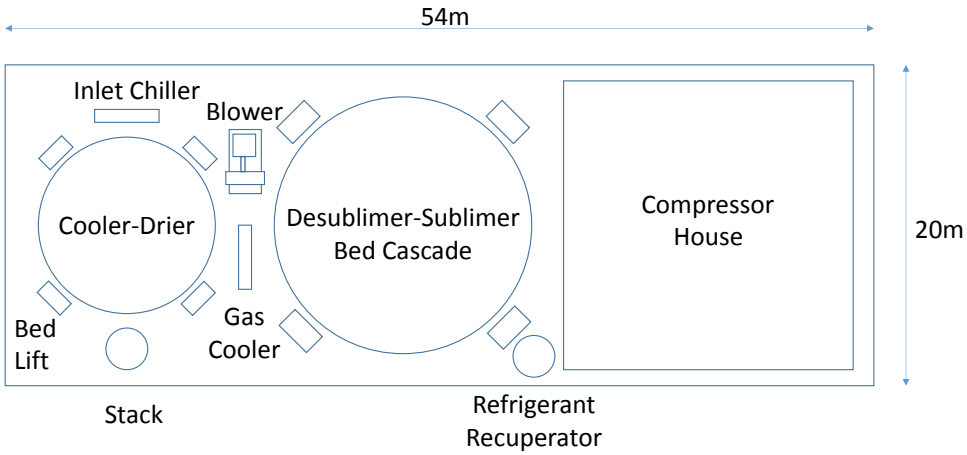

Fig. 3. Indicative arrangement for the A3C CO_2 process applied to the oil-fired boiler application.

The estimates of power and utility consumption for the various elements of the A3C process are shown in Table 8. These were derived from the Aspen modelling and from calculations of system pressure drops based on bed superficial gas velocities of 70% of that necessary for fluidisation. The total pressure drop lies in the range 100-150 mbar.

Table 8: The energy consumption of the main elements for A3C in the three applications

Main electrical power consumers	Units	Oil-fired Boiler	CCGT	Biogas Upgrading
Inlet and part lean bed chiller	MW	1.0	1.1	0.0035
Refrigeration compressor	MW	21.6	13.0	0.076
Booster fan	MW	1.9	1.0	0.0007
Bed transfer conveyors	MW	0.5	0.2	0.0006
CO_2 delivery compressor	MW	9.37	1.87	0.042
Total	MW	34.4	17.2	0.122
Total specific energy of CO_2 capture	kWh/tonne	332	831	263
Specific energy of CO_2 separation	kWh/tonne	241	741	172
Cooling water utility requirement	MW	34	17	0.12

Following the preliminary engineering step, the costs of the various elements were estimated as described above. While the conventional exchangers were costed using the cost estimation tools of AspenPlus®, the fluid to bed and direct bed to gas heat exchangers were costed by analogy with shell and tube heat exchangers with a single pass on the shell side and by costs for packed columns respectively. Table 9 shows the equipment and installation costs for the three A3C cases evaluated.

Table 9: A3C equipment cost estimates

Equipment costs £k	Oil-fired boiler	CCGT	Biogas upgrading
Core fridge			
Conventional HX	255	345	8.5
Fluid to bed HX	1,539	640	32.9
Direct bed to gas HX	150	67	3.9
Refrigeration compressor system	11,809	6,554	100
CO_2 Compressor system	12,422	2,590	83
Cooler-drier			
Fluid to bed HX	215	78	8.6
Direct bed to gas HX	304	260	7.4
Inlet chiller and HX	550	172	3.9
Balance of plant			
Core process bed conveyors	500	500	10
Total Direct Equipment Cost	27,744	11,206	258.1
Circulating bed material	2,641	1,367	7.2

Applying the methodology detailed in Table 2, the total capital requirement is derived in Table 10.

Table 10: A3C project and total capital requirement estimates

Cost Element £k	Oil-fired boiler	CCGT	Biogas upgrading
Total DEC	27,744	11,206	258
Total fixed capital investment	69,170	27,938	545.2
Start-up and bed material	6,917	2,794	54.5
Interest during construction	6,163	2,489	48.5
Total Capital Requirement	82,250	33,221	648.2

3.4. Benchmarking of the A3C process

The LCCC model compared the A3C process with the reference MEA system for a range of heat and power costs, with a baseline assumption that the steam would otherwise be used to generate

electricity in a steam turbine. Table 11 compares the three applications using the A3C process and the reference MEA cases. This demonstrates that the initial A3C process designs can offer comparable or lower costs to the mature MEA process for the larger applications. However, the A3C process is radically better than MEA for the biogas upgrading case due to its lower capital and operating costs.

Table 11: Comparison of LCCC for MEA and A3C for the different applications at baseline energy cost

	Utility Boiler		CCGT		Biogas Upgrading	
	MEA	A3C	MEA	A3C	MEA	A3C
Heat (MJ/s)	114	0	28.6	0	0.49	0
Power (MW)	12.2	34.4	2.95	17.2	0.06	0.12
Equivalent Power (MWe)	38.6	34.4	9.9	17.2	0.18	0.12
Capex (£m)	81.3	82.3	37.5	33.2	4.9	0.65
Opex excl. energy (£m)	6.4	5.1	3.6	1.6	0.69	0.25
LCCC (£/te CO_2)	39.7	34.9	76.8	79.3	395.8	120.9

While the LCCC analysis above, with its initial assumptions, provides one measure to benchmark A3C against MEA there are several other perspectives on the comparison that are useful to consider.

Firstly, examination of the main components of the LCCC will reveal more about the advantages or otherwise of A3C. It is apparent that A3C offers a lower capital cost than MEA for each application, which is significant, given the uncertainty in estimation, only for the biogas case. Here it seems that A3C benefits from more attractive costs at smaller scale, although it may also be that the Aspen cost estimations for the reference case are somewhat pessimistic at such a small scale of plant.

A second area of advantage for A3C is in non-energy operating cost. The different methods of estimating operational manning applied to the two technologies weaken the validity of this comparison, but it is true that a purely mechanical and thermal process is likely to require less supervision than a chemical absorption process. Further work for real plant applications will be necessary to establish a firmer basis for comparison for such costs.

The final element of the LCCC comparison is the cost of energy consumption. The relative energy consumption of the processes does not show a consistent trend across the applications, suggesting that the A3C process conditions have not been well adjusted in each case. A better understanding of operation of the A3C process across a wider range of applications, by scale and CO_2 concentration, is necessary to obtain a more robust comparison.

The processes may also be compared by physical features. The diameter of vessels used by A3C and MEA are comparable, since the gas-side loading of the columns and beds are similar. However, the intensive heat transfer employed in the A3C process means that the process vessels are less tall. It is possible that the weight of the vessels for the A3C process will be greater due to the higher specific gravity of the bed material than amine solution. The A3C process includes fewer pumps and blowers than the MEA process but includes mechanical handling equipment to move the bed. The lack of process consumables or facilities for absorbent regeneration for the A3C process means that it is simpler, requires less space for access and has reduced requirements for managing the HSE risks of process chemicals.

A final basis for benchmarking the processes is their relative technological readiness. As might be anticipated, the A3C process is only at TRL level 2 or 3 (proof of principle and initial demonstration), while the MEA process is at TRL 9 (proven in commercial application). This means that while A3C may benefit from further process optimization and development, it also faces risks of unforeseen technical or cost issues which could reduce its viability compared with the proven MEA technology.

4. Conclusions

This work has presented a novel cryogenic process modelled using the built-in Aspen Plus® model components adapted to represent unconventional processes involving solid formation at cryogenic conditions. The A3C process has been shown to be feasible for a range of scales and CO_2 concentrations in the process gas streams. The techno-economic evaluation of the A3C process has shown comparable costs with the reference mature MEA technology for the larger selected applications, and significantly lower costs in the smaller application. The selection of the A3C process over MEA may depend on the local availability and cost of heat, electricity and/or cooling water. It should be noted that A3C is an immature technology and while extensive regenerative energy recovery has been used, there are significant opportunities for further improvement and optimization with additional potential for trade-offs between energy consumption and capital cost. This work confirms assessments by others (Clodic et al., 2005a; Pellegrini et al., 2018) that cryogenic separation processes can offer significant advantages over alternatives in biogas applications. The A3C process offers advantages of simplicity and avoidance of gas compression processes compared with the alternatives for biogas upgrading. Limited research is being done on cryogenic separation compared with more mature separation processes and this needs to be increased to explore and exploit the potential benefits.

Acknowledgements

The authors thank Innovate UK for funding the A3C Carbon Capture Project Ref.132957, and industrial collaborators Anthony Alderson (WSP), Andrew Williams (DNV GL) and Dr Bryony Livesey (Costain) for their support.

References

Achenbach, E., 1995. Heat and flow characteristics of packed beds. Experimental Thermal and Fluid Science 10, 17-27.

Agbonghae, E.O., Hughes, K.J., Ingham, D.B., Ma, L., Pourkashanian, M., 2014. Optimal Process Design of Commercial-Scale Amine-Based CO2 Capture Plants. Industrial & Engineering Chemistry Research 53, 14815-14829.

Akram, M., Ali, U., Best, T., Blakey, S., Finney, K.N., Pourkashanian, M., 2016. Performance evaluation of PACT Pilot-plant for CO2 capture from gas turbines with Exhaust Gas Recycle. International Journal of Greenhouse Gas Control 47, 137 - 150.

Albrecht, F.G., König, D.H., Baucks, N., Dietrich, R.U., 2017. A standardized methodology for the techno-economic evaluation of alternative fuels – A case study. Fuel 194, 511-526.

Alhajaj, A., Mac Dowell, N., Shah, N., 2016. A techno-economic analysis of post-combustion CO2capture and compression applied to a combined cycle gas turbine: Part II. Identifying the cost-optimal control and design variables. International Journal of Greenhouse Gas Control 52, 331-343.

BEIS, 2018. Assessing the Cost Reduction Potential and Competitiveness of Novel (Next Generation) UK Carbon Capture Technology Benchmarking State-of-the-art and Next Generation Technologies.

Berstad, D., Anantharaman, R., Nekså, P., 2013. Low-temperature CO_2 capture technologies – Applications and potential. International Journal of Refrigeration 36, 1403-1416.

Billet, R., Schultes, M., 1993. Predicting mass transfer in packed columns. Chemical Engineering & Technology 16, 1-9.

Burt, S., Baxter, A., Baxter, L., 2009. Cryogenic CO2 Capture to Control Climate Change Emissions.

Chauvel Alain, L.P.B.Y.R.C.A.J.-P., 1976. Manual of Economic Analysis of Chemical Processes, 1 ed. McGraw-Hili, Inc, Paris.

Clodic, D., El Hitti, R., Younes, M., Bill, A., Casier, F., 2005a. CO_2 capture by anti-sublimation - thermo-economic process evaluation, Fourth Annual Conference on Carbon Capture Sequestration, Alexandria, USA.

Clodic, D., Younes, M., 2002. A new method for CO_2 capture: frosting CO_2 at atmospheric pressure, Sixth International Conference on Greenhouse Gas Control Technologies, GHGT, Kyoto.

Clodic, D., Younes, M., Bill, A., 2005b. Test results of CO_2 capture by anti-sublimation, Capture efficiency and energy consumption for boiler plants, 8th International Conference on Greenhouse Gas Control Technologies (GHGT-8), Trondheim, Norway.

Clodic, D., Younes, M., Riachi, Y., El Hitti, R., 2011. CO_2 capture by antisublimation using integrated cascade system, 3rd IIR International Congress of Refrigeration, Prague, Czech Republic.

Colakyan, M., 1985. Moving bed heat transfer and fluidized elutriation. Oregon State University.

Couper, J.R., 2003. Process Engineering Economics. CRC Press.

Davidson, R.M., 2007. Post-combustion carbon capture from coal fired plants - solvent scrubbing. IEA Clean Coal Centre, London.

Diego, M.E., Bellas, J.-M., Pourkashanian, M., 2018. Techno-economic analysis of a hybrid CO2 capture system for natural gas combined cycles with selective exhaust gas recirculation. Applied Energy 215, 778-791.

Don Valley Engineering, L., 2018. Process Plant for the Maltings Industry.

Gouedard, C., Picq, D., Launay, F., Carrette, P.L., 2012. Amine degradation in CO2 capture. I. A review. International Journal of Greenhouse Gas Control 10, 244-270.

Husebye, J., Brunsvold, A.L., Roussanaly, S., Zhang, X., 2012. Techno Economic Evaluation of Amine based CO2 Capture: Impact of CO2 Concentration and Steam Supply. Energy Procedia 23, 381-390.

IEAGHG, 2011. Rotating equipment for carbon dioxide capture and storage.

Iijima, M., 1998. A Feasible New Flue Gas CO2 Recovery Technology for Enhanced Oil Recovery. Proceedings of SPE/DOE Improved Oil Recovery Symposium 333.

Jäger, A., Span, R., 2012. Equation of State for Solid Carbon Dioxide Based on the Gibbs Free Energy. Journal of Chemical & Engineering Data 57, 590-597.

Jung, J., Jeong, Y.S., Lim, Y., Lee, C.S., Han, C., 2013. Advanced CO2 Capture Process Using MEA Scrubbing: Configuration of a Split Flow and Phase Separation Heat Exchanger. Energy Procedia 37, 1778-1784.

Knudsen, J.N., Jensen, J.N., Vilhelmsen, P.-J., Biede, O., 2009. Experience with CO2 capture from coal flue gas in pilot-scale: Testing of different amine solvents. Energy Procedia 1, 783-790.

Lemmon, E.W., McLinden, M.O., Friend, D.G., 2018. Thermophysical Properties of Fluid Systems, in: Linstrom, P.J., Mallard, W.G. (Eds.), NIST Chemistry WebBook, NIST Standard Reference Database. National Institute of Standards and Technology, Gaithersburg.

Metz, B., Davidson, O., de Coninck, H., Loos, M., Meyer, L., 2005. IPCC Special Report on Carbon Dioxide Capture and Storage. Working Group III of the Intergovernmental Panel on Climate Change.

Nwaoha, C., Smith, D.W., Idem, R., Tontiwachwuthikul, P., 2018. Process simulation and parametric sensitivity study of CO2 capture from 115 MW coal–fired power plant using MEA–DEA blend. International Journal of Greenhouse Gas Control 76, 1-11.

Peeters, A.N.M., Faaij, A.P.C., Turkenburg, W.C., 2007. Techno-economic analysis of natural gas combined cycles with post-combustion CO2absorption, including a detailed evaluation of the development potential. International Journal of Greenhouse Gas Control 1, 396-417.

Pellegrini, L.A., De Guido, G., Langé, S., 2018. Biogas to liquefied biomethane via cryogenic upgrading technologies. Renewable Energy 124, 75-83.

Peters, M.S., Timmerhaus, K.D., 1991. Plant design and economics for chemical engineers. McGraw-Hil.

Podtcherniaev, O., Boiarski, M., Lunin, A., 2002. Comparative Performance Of Two-Stage Cascade And Mixed Refrigerant Systems In A Temperature Range From –100C To –70C, International Refrigeration and Air Conditioning Conference, USA.

Rabensteiner, M., Kinger, G., Koller, M., Gronald, G., Hochenauer, C., 2014. Pilot plant study of ethylenediamine as a solvent for post combustion carbon dioxide capture and comparison to monoethanolamine. International Journal of Greenhouse Gas Control 27, 1-14.

Rao, A.B., Rubin, E.S., Berkenpas, M., 2004. An integrated modeling framework for carbon management technologies.

Roussanaly, S., Fu, C., Voldsund, M., Anantharaman, R., Spinelli, M., Romano, M., 2017. Techno-economic Analysis of MEA CO2 Capture from a Cement Kiln – Impact of Steam Supply Scenario. Energy Procedia 114, 6229-6239.

Rubin, E.S., Short, C., Booras, G., Davison, J., Ekstrom, C., Matuszewski, M., McCoy, S., 2013. A proposed methodology for CO2 capture and storage cost estimates. International Journal of Greenhouse Gas Control 17, 488-503.

Schach, M.-O., Oyarzún, B., Schramm, H., Schneider, R., Repke, J.-U., 2011. Feasibility study of CO2 capture by anti-sublimation. Energy Procedia 4, 1403-1410.

Seibert, F., Chen, E., Perry, M., Briggs, S., Montgomery, R., Rochelle, G., 2011. UT/SRP CO2 capture pilot plant — Operating experience and procedures. Energy Procedia 4, 1616-1623.

Sexton, A., Dombrowski, K., Nielsen, P., Rochelle, G., Fisher, K., Youngerman, J., Chen, E., Singh, P., Davison, J., 2014. Evaluation of reclaimer sludge disposal from post-combustion CO2 Capture. Energy Procedia 63, 926-939.

Song, C., Liu, Q., Ji, N., Deng, S., Zhao, J., Kitamura, Y., 2017. Advanced cryogenic CO2 capture process based on Stirling coolers by heat integration. Applied Thermal Engineering 114, 887-895.

Song, C.F., Kitamura, Y., Li, S.H., Jiang, W.Z., 2012. Parametric Analysis of a Novel Cryogenic CO2 Capture System Based on Stirling Coolers. Environmental Science & Technology 46, 12735-12741.

Stéphenne, K., 2014. Start-up of World's First Commercial Post-combustion Coal Fired CCS Project: Contribution of Shell Cansolv to SaskPower Boundary Dam ICCS Project. Energy Procedia 63, 6106-6110.

Strazisar, B.R., Anderson, R.R., White, C.M., 2003. Degradation Pathways for Monoethanolamine in a CO2 Capture Facility. Energy & Fuels 17, 1034-1039.

Towler, G., Sinnott, R., 2013a. Capital Cost Estimating, in: Towler, G., Sinnott, R. (Eds.), 2 ed. Butterworth-Heinemann, Boston, pp. 307-354.

Towler, G., Sinnott, R., 2013b. Economic Evaluation of Projects, in: Towler, G., Sinnott, R. (Eds.), 2 ed. Butterworth-Heinemann, Boston, pp. 389-429.

Tuinier, M.J., Hamers, H.P., van Sint Annaland, M., 2011a. Techno-economic evaluation of cryogenic CO_2 capture—A comparison with absorption and membrane technology. International Journal of Greenhouse Gas Control 5, 1559-1565.

Tuinier, M.J., van Sint Annaland, M., Kramer, G.J., Kuipers, J.A.M., 2010. Cryogenic CO_2 capture using dynamically operated packed beds. Chemical Engineering Science 65, 114-119.

Tuinier, M.J., van Sint Annaland, M., Kuipers, J.A.M., 2011b. A novel process for cryogenic CO2 capture using dynamically operated packed beds—An experimental and numerical study. International Journal of Greenhouse Gas Control 5, 694-701.

Turton, R., 2009. Analysis, Synthesis, and Design of Chemical Processes. Pearson Education, Inc.

Vattenfall, A.S., 2008. Reference cases and guidelines for technology concepts, pp. 1-49.